ELSEVIER

Physica E 10 (2001) 362–367

PHYSICA E

www.elsevier.nl/locate/physe

Magneto-photoluminescence studies of Cd(Mn)Se/Zn(Mn)Se diluted magnetic nanostructures

A.A. Toropov[a,*], S.V. Sorokin[a], K.A. Kuritsyn[a], S.V. Ivanov[a], G. Pozina[b], J.P. Bergman[b], Mt. Wagner[b], W.M. Chen[b], B. Monemar[b], A. Waag[c], D.R. Yakovlev[a,d], C. Sas[d], W. Ossau[d], G. Landwehr[d]

[a] *A.F. Ioffe Physico-Technical Institute of RAS, Politeknitcheskaya 26, St. Petersburg 194021, Russia*
[b] *Department of Physics and Measurement Technology, University of Linköping, S-581 83 Linköping, Sweden*
[c] *Abteilung Halbleiterphysik, Universität Ulm, 89081 Ulm, Germany*
[d] *Physikalisches Institute der Universität Würzburg, D-97074 Würzburg, Germany*

Abstract

We report on cw and time-resolved photoluminescence (PL) studies of Cd(Mn)Se/Zn(Mn)Se diluted magnetic semiconductor nanostructures grown by molecular beam epitaxy. Excitonic PL intensity, decay time and Zeeman splitting have been studied systematically as a function of Cd(Mn)Se nominal thickness, Mn concentration and sample design. Wave function mapping has been performed, evidencing the formation of semi-magnetic quantum disk islands in the samples with thick enough Cd(Mn)Se insertions.

PACS: 75.50.Pp; 78.20.Ls

Keywords: CdMnSe nanostructures; Quantum dots; Diluted magnetic semiconductors

The CdSe/ZnSe heteropair is known as a useful system for fabrication of nanostructures for blue-green optoelectronic applications [1]. Both quantum wells (QWs) and self-assembled quantum dots (QDs) can be grown by molecular beam epitaxy (MBE) in this system, depending on the nominal thickness of the evaporated CdSe insertion [1–4]. On the other hand, increasing attention has been recently given to diluted magnetic semiconductor (DMS) heterostructures due to the potential optoelectronic and magnetoelectronic applications based on spin-polarized transport of carriers [5]. Further expectations concern the studies of electronic spin behavior in zero-dimensional (0D) magnetic structures with a discretized electronic system. In this context, the recently demonstrated formation of semimagnetic nanostructures due to the incorporation of Mn^{2+} ions

* Corresponding author. Tel.: +7-812-247-9124; fax: +7-812-247-8640.
E-mail address: toropov@beam.ioffe.rssi.ru (A.A. Toropov).

1386-9477/01/$ - see front matter
PII: S1386-9477(01)00117-5

in CdSe/ZnSe strained heterostructures [6–8] looks particularly promising. In this paper, we report on cw and time-resolved magneto-photoluminescence (PL) properties of Cd(Mn)Se/Zn(Mn)Se structures grown by MBE. Excitonic PL line intensity, energy position and decay time have been studied as a function of magnetic field, Cd(Mn)Se nominal thickness, Mn concentration and sample design.

Three types of samples (A, B and C) have been grown by MBE pseudomorphically on (0 0 1) GaAs substrates. The type A structures include a single CdSe layer embeded in a 20 nm thick $Zn_{1-x}Mn_xSe$ DMS layer. Additional ZnSe non-magnetic spacers are inserted around the CdSe well in the type B samples, keeping constant the whole thickness of a non-magnetic region. The type C structures are $Cd_{1-x}Mn_xSe$ layers embedded in pure ZnSe. Fig. 1 displays a schematic drawing of all three types of samples. The described structures are surrounded by thick ZnBeSe barriers lattice-matched to GaAs. Within each type, the samples differ mainly in the nominal thickness of the Cd(Mn)Se layer and Mn concentration. In this paper, we focus on the properties of the following samples. Three samples of type A are A_0.4_0.11 (the label A_w_x specifies the type A structure as a CdSe layer with nominal thickness w measured in monolayers (MLs) of strained CdSe, surrounded by $Zn_{1-x}Mn_xSe$), A_1.0_0.11, and A_2.0_0.11. Four samples of type B are B_0.5_1.85_0.11, B_1.0_1.75_0.11, B_2.0_1.6_0.11, and B_2.8_1.5_0.11. The sample label B_w1_w2_x means a CdSe layer with nominal thickness of w1 (ML), surrounded successively by w2 (nm) thick ZnSe spacers and $Zn_{1-x}Mn_xSe$. Type C samples are C_1.5_0.07 and C_1.5_0.15. Here C_w_x means a type C sample with a $Cd_{1-x}Mn_xSe$ layer of nominal thickness w (ML) embedded in ZnSe.

Magneto-PL measurements were carried out in Faraday geometry in an He cryostat with a superconducting magnet at 1.6–1.9 K. A linearly polarized emission of a UV cw Ar^+ laser was used for cw PL measurements. Time-resolved (TR) PL measurements were performed with a frequency-doubled beam of a mode-locked Ti/Sapphire laser and a Hamamatsu streak camera. The setup time resolution is estimated as 15–20 ps. Either the σ^+ or σ^- component of the PL was selected by a quarter-λ plate coupled with a linear polarizer.

All the samples demonstrate bright excitonic PL at low temperature. The zero-field spectral position and width of the PL lines are mainly determined by the nominal thickness of Cd(Mn)Se layers. The increase in thickness results in a red shift and broadening of the line, in qualitative agreement with the results obtained previously in non-magnetic CdSe/ZnSe structures [4]. For all types of structures, the PL decay time is found to depend strongly on Mn concentration and on the relative probability of an electron and hole to be within the magnetic area. Very fast decay times $\sim$ 15 ps (close to the setup time resolution) are observed in type A samples characterized by near 100% overlap of electron and hole wave functions with the $Zn_{0.89}Mn_{0.11}Se$ DMS barriers. The strong interaction of the wave functions with DMS regions in these samples is governed by a relatively weak carriers localization by the ultra-thin CdSe layers and possible diffusion of Mn atoms from the DMS barriers into the intentionally non-magnetic CdSe layers.

Longer decay times (20–70 ps) are observed in the type C samples, which can be explained by a smaller overlap of the wave functions, spreading deep in the non-magnetic barriers, with a narrow sheet of CdMnSe. The suppressive effect of the Mn^{2+} ions can be clearly seen by comparing $\sim$ 20 and $\sim$ 60 ps decay times observed in the samples C_1.5_0.15 and C_1.5_0.07, respectively. Even longer decay times (up to 200 ps) are observed in the type B samples, where only wave function tails interact with DMS $Zn_{0.89}Mn_{0.11}Se$ barriers, penetrating there through non-magnetic ZnSe spacers. The decay curves in these samples are not single-exponential and the decay time varies significantly within the PL line contour, increasing at longer wavelengths. Note that such TR PL properties are very close to those of the respective non-magnetic CdSe/ZnSe samples [4]. All together these findings indicate the existence of an efficient channel for non-radiative recombination in the samples, connected with the incorporated Mn^{2+} ions.

Application of a magnetic field influences the PL decay behavior, elongating the decay times. An example of this action is illustrated in Fig. 2 by two σ^+ PL decay curves measured in C_1.5_0.15 at 0 and 5 T. Both curves can be reasonably fitted by a two-exponential decay model, as shown in Fig. 2 by dashed lines. The magnetic field increases the decay times and enhances

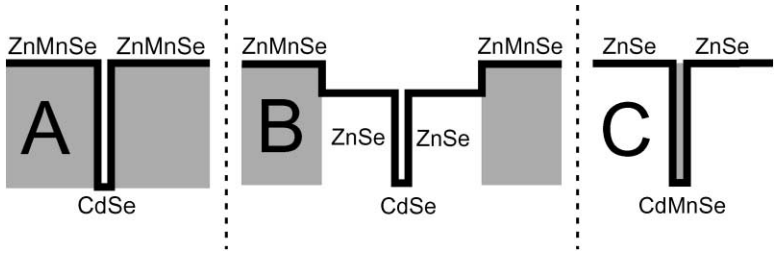

Fig. 1. Schematic drawing of the samples.

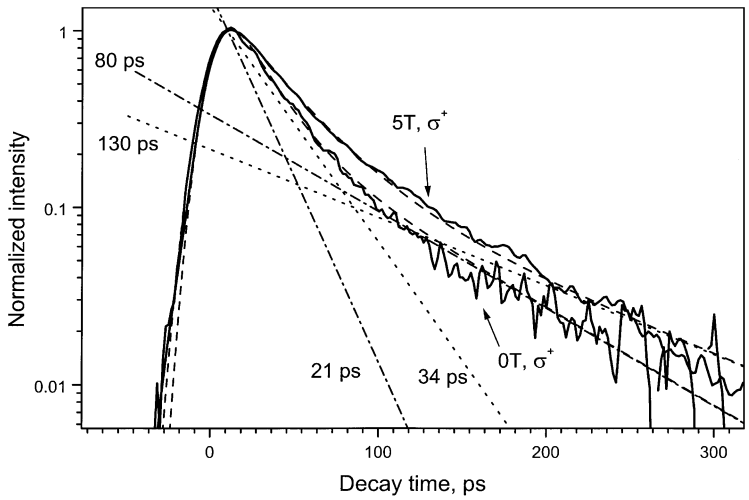

Fig. 2. Spectrally integrated σ^+ PL decay curves measured in C_1.5_0.15 at 0 and 5 T. Solid curves present experimental data, dashed curves show the results of fitting by a two-exponential decay model. Dotted and dash–dotted lines illustrate contributions from the two decay components for 5 and 0 T decay curves, respectively.

the relative contribution of the slow decaying component. Fig. 3 illustrates the latter effect for the samples A_0.4_0.11, A_1.0_0.11, A_2.0_0.11 and C_1.5_0.15, displaying 5 T σ^+ PL spectra, both time-integrated and extracted from the two-exponential decay fitting separately for the fast and slow decaying components. Note that no contribution from the "slow" PL component could be detected in the type A samples at zero magnetic field. Also, the sample A_0.4_0.11 with the thinnest CdSe layer does not exhibit the "slow" PL at any fields and polarizations. The slow decaying σ^+PL, although weak, is quite noticeable in the sample A_1.0_0.11 at 5 T. It is even stronger in the sample A_2.0_0.11 and is especially well seen in the sample C_1.5_0.15. Analyzing the spectra in Fig. 3, one can notice the clear dependence of the relative intensity of the "slow" component on the PL peak inhomogeneous width which can be regarded as a measure of the layer intrinsic disordering. The more is the layer structural inhomogeneity, the larger is the "slow" PL relative contribution.

Recently, it has been demonstrated by high resolution transmission electron microscopy that the CdSe/ZnSe structures thicker then 1 ML are in fact ZnCdSe layers comprising flat islands (quantum disks) with an enlarged content of Cd [9]. Our results are in good agreement with this description. Really, the enhanced localization of carrier wave functions within the Cd-rich islands modifies their overlap with the DMS regions, thus resulting in the emergence

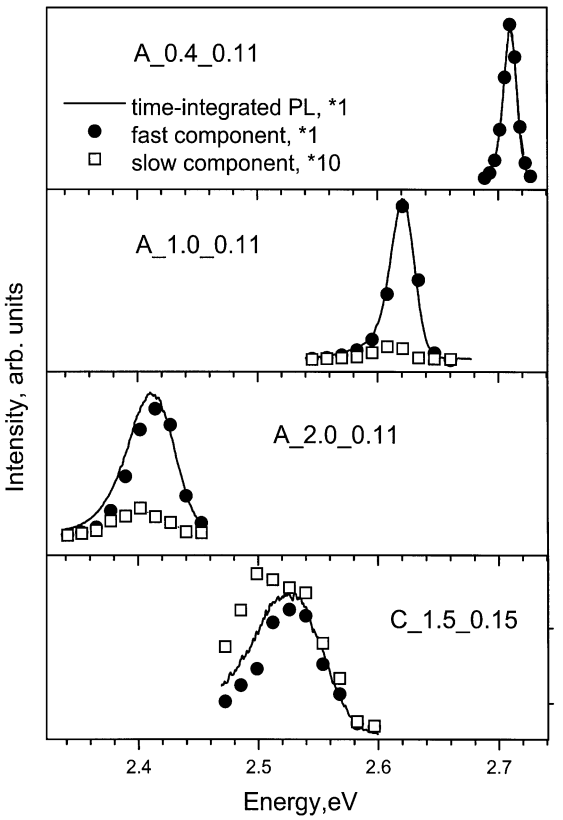

Fig. 3. Spectra of time-integrated PL (solid curves), fast PL decay component (circles) and slow PL decay component (squires), measured in the samples A_0.4_0.11, A_1.0_0.11, A_2.0.0.11 and C_1.5_0.15.

of regions with different rates of non-radiative recombination. The inhomogeneous lateral distribution of Mn^{2+} ions is also very probable, especially in the type C samples. In-plane localization action of the magnetic field applied in the Faraday geometry prevents tunneling and diffusive migration of carriers between the regions, revealing slower decaying PL from the areas with lower rates of non-radiative recombination.

For all the samples, an increase in magnetic field results in a drastic enhancement (about one order of magnitude) of the PL intensity. This observation was also reported by Kim et al. [7], who detected a magnetic field induced increase in the integral intensity of the excitonic emission from CdSe/(Zn,Mn)Se nanostructures, accompanied by quenching of the emission band (near 2.0 eV) related to Mn inter-shell transitions. Owing to this observation, the authors of Ref. [7] explained the effect in terms of an efficient transfer of excitations between the excitons and the Mn^{2+} ions, which is suppressed by a magnetic field. Among the samples studied in this paper, similar behavior was observed only in the type C samples, particularly in C_1.5_0.15. No influence of a magnetic field on the intensity of the 2.0 eV PL line was detected in the type A samples. Behavior similar to type A samples has been reported recently for ZnMnSe/ZnBeMgSe QWs [10]. No reliable conclusions can be made concerning the type B samples, because the 2.0 eV emission band there is very weak.

The observed diversity reflects the existence of different mechanisms contributing to the effect of the field-induced increase in the excitonic PL intensity, whose relative contributions depend on the sample properties. For the structures characterized by lateral inhomogeneity, the effect can be partly explained by the localization action of the magnetic field on the carriers wave functions, preventing their penetration into the regions with enhanced non-radiative recombination. The importance of this effect, at least for certain samples, is confirmed by the above analysis of the PL decay behavior. However, neither this scheme, nor the mechanism suggested by Kim et al. [7] can explain the observed near one order of magnitude increase in the PL intensity in the sample A_0.4_0.11, where the Mn^{2+} related line is field-independent and the decay curves are practically not affected by the magnetic field.

Finally, we consider the effect of giant Zeeman splitting of excitons, which is revealed in the samples as a large red shift of the excitonic PL line and its almost 100% σ^+ polarization even at small fields less then 1 T. Observation of this effect has provided an excellent opportunity for "mapping" the wave function distribution in nanostructures of various geometries [11]. For this purpose, we choose the set of type B samples, for two reasons. Firstly, there is no direct contact of Mn ions with the CdSe/ZnSe active region whose intrinsic structure is currently well documented for a wide range of CdSe nominal thicknesses [9,12,13]. Secondly, for this type of samples, the influence of the Mn diffusion along the growth axis on the giant Zeeman splitting is minimal and can be neglected in calculations. Fig. 4 demonstrates the PL shift ΔE_g versus magnetic field for the four type B samples. The solid

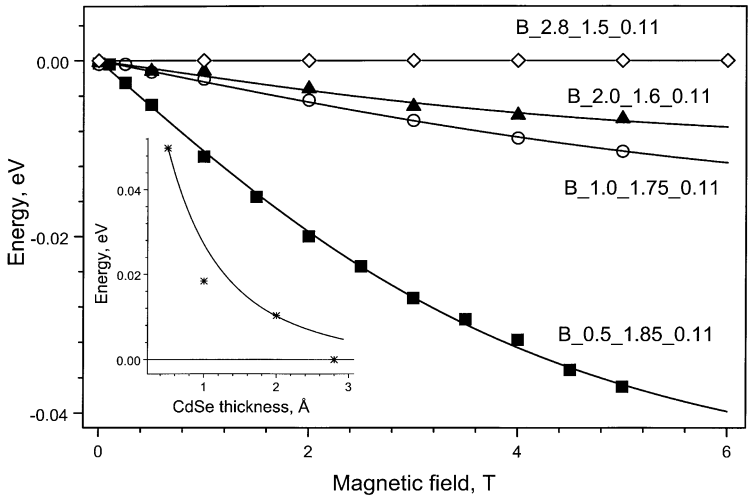

Fig. 4. Energy shifts of the PL line versus magnetic field for type B samples. Symbols show experimental data, solid curves represent the fits. The inset shows the saturation band edge shift versus CdSe layer nominal thickness as measured (asterisks) and calculated (solid curve) in type B samples.

curves represent the fits performed using the conventional description of the giant Zeeman splitting by a mean-field approximation [14],

$$\Delta E_g = \Delta E_{g0}\langle S_z\rangle,$$

where ΔE_{g0} is the saturation value of the shift and $\langle S_z\rangle$ is the mean spin of the Mn^{2+} ions, expressed through the modified Brillouin function [14]. Fig. 4 displays the obtained values of the fitting parameter ΔE_{g0} plotted as a function of the nominal thickness of the CdSe layer. The band edge shift decreases with an increase in the CdSe thickness, which reflects enhanced localization of the carrier wave functions along the growth axis and hence their smaller overlap with DMS regions. No shift at all was detected for the sample B_2.8_1.5_0.11 with the thickest CdSe layer. To model this curve, we calculated ΔE_{g0} as a sum of the conduction band and valence band shifts estimated as the respective exchange constants multiplied by the coefficients proportional to the overlap of the probability $|\Psi_i|^2$ of the states with the DMS layers [11]. The electron and hole envelope wave functions, Ψ_c and Ψ_v, are calculated in the simplest two-band effective-mass scheme, modeling the CdSe/ZnSe layers as a laterally homogeneous graded-gap ZnCdSe QW. The Cd distribution profile along the structure growth axis was estimated from the X-ray diffraction studies of CdSe/ZnSe superlattices [12,13]. The calculated curve (solid curve in the inset in Fig. 4) is normalized to match the ΔE_{g0} value obtained for the sample B_0.5_1.85_0.11 with the thinnest CdSe layer. The curve satisfactorily describes the experimental data, except for the noticeable overestimation for the thickest layer. The possible explanation of the discrepancy can be the additional localization of the wave functions in Cd rich quantum disk islands typical for the thick enough CdSe/ZnSe layers [9], which results in a negligible overlap of the wave function tails with the DMS barriers.

In conclusion, we have studied excitonic magneto-PL properties of Cd(Mn)Se/Zn(Mn)Se nanostructures with different geometries and Mn distributions. It has been found that the PL life-time varies in the range of 15–200 ps among the samples, depending on the carriers probability to be within the DMS region and the Mn^{2+} ions concentration. Especially useful for spin-device applications can be the samples with accurately designed non-magnetic spacers separating the CdSe insertion and the ZnMnSe DMS barriers. In such samples, relatively long exciton lifetimes (up to 200 ps) coexist with a pronounced giant Zeeman splitting, which allows one to obtain a large net concentration of spin-polarized carriers at relatively small magnetic fields. Wave function mapping has

been performed for the samples of this type, revealing enhanced carriers localization in the structures with thick enough CdSe. The latter observation evidences, most probably the formation of Cd rich quantum disk islands in the semi-magnetic structures.

Acknowledgements

This work was supported in part by RFBR Grant No. 00-02-16997a, Volkswagen-Stiftung, INTAS grant No. 97-31907, Deutsche Forschungsgemeinschaft (SFB 410) and the Royal Swedish Academy of Sciences.

References

[1] S.V. Ivanov, A.A. Toropov, S.V. Sorokin, T.V. Shubina, I.V. Sedova, A.A. Sitnikova, P.S. Kopév, Zh.I. Alferov, H.-J. Lugauer, G. Reuscher, M. Keim, F. Fischer, A. Waag, G. Landwehr, Appl. Phys. Lett. 74 (1999) 498.
[2] F. Flack, N. Samarth, V. Nikitin, P.A. Crowell, J. Shi, J. Levy, D.D. Awschalom, Phys. Rev. B 54 (1996) 17312.
[3] F. Gindele, U. Woggon, W. Langbein, J.M. Hwam, K. Leonardi, K. Ohkawa, D. Hommel, J. Crystal Growth 184/185 (1998) 306.
[4] S.V. Ivanov, A.A. Toropov, T.V. Shubina, S.V. Sorokin, A.V. Lebedev, I.V.Sedova, P.S. Kopév, G.R. Pozina, J.P. Bergman, B. Monemar, J. Appl. Phys. 83 (1998) 3168.
[5] R. Fiederling, M. Keim, G. Reuscher, W. Ossau, G. Schmidt, A. Waag, L.W. Molenkamp, Nature 402 (1999) 787.
[6] P.A. Crowell, V. Nikitin, J.A. Gupta, D.D. Awschalom, F. Flack, N. Samarth, Physica E 2 (1998) 854.
[7] C.S. Kim, M. Kim, S. Lee, J. Kossut, J.K. Furdyna, M. Dobrowolska, J. Crystal Growth 214/215 (2000) 395.
[8] A.A. Toropov, S.V. Sorokin, K.A. Kuritsyn, S.V. Ivanov, P.S. Kopév, G. Reuscher, A. Waag, M. Wagner, W.M. Chen, B. Monemar, Proceedings of Eighth International Symposium "Nanostructures: physics and Technology", St. Petersburg, Russia, 19–23, June 2000, p. 440.
[9] N. Peranio, A. Rosenauer, D. Gerthsen, S.V. Sorokin, I.V. Sedova, S.V. Ivanov, Phys. Rev. B 61 (2000) 1605.
[10] B. König, U. Zehnder, D.R. Yakovlev, W. Ossau, T. Gerhard, M. Keim, A. Waag, G. Landwehr, Phys. Rev. B 60 (1999) 2653.
[11] S. Lee, M. Dobrowolska, J.K. Furdyna, L.R. Ram-Mohan, Phys. Rev. B 59 (1999) 10302.
[12] R.N. Kyutt, A.A. Toropov, S.V. Sorokin, T.V. Shubina, S.V. Ivanov, M. Karlsteen, M. Willander, Appl. Phys. Lett. 75 (1999) 373.
[13] A.A. Toropov, T.V. Shubina, R.N. Kyutt, S.V. Sorokin, S.V. Ivanov, D.L. Fedorov, M. Karlsteen, M. Willander, Phys. Stat. Sol. A 178 (2000) 203.
[14] J.A. Gaj, R. Planel, G. Fishman, Solid State Commun. 29 (1979) 435.